Cancer Letters 349 (2014) 144–151

Contents lists available at ScienceDirect

Cancer Letters

journal homepage: www.elsevier.com/locate/canlet

Inhibiting glucosylceramide synthase facilitates the radiosensitizing effects of vinorelbine in lung adenocarcinoma cells

Wei-Hsin Chiu [a,b], Helen Hai-Wen Chen [c], Jang-Yang Chang [a,d], Sheng-Jie Luo [a], Chia-Ling Li [a], Chia-Ling Chen [e], Wu-Chou Su [b,f,*], Chiou-Feng Lin [a,e,f,g,*]

[a] Institute of Clinical Medicine, College of Medicine, National Cheng Kung University, Tainan, Taiwan
[b] Division of Hemato-Oncology, Department of Internal Medicine, National Cheng Kung University Hospital, Tainan, Taiwan
[c] Department of Radiation Oncology, National Cheng Kung University Hospital, Tainan, Taiwan
[d] National Institute of Cancer Research, National Health Research Institutes, Tainan, Taiwan
[e] Department of Microbiology and Immunology, College of Medicine, National Cheng Kung University, Tainan, Taiwan
[f] Institute of Basic Medical Sciences, College of Medicine, National Cheng Kung University, Tainan, Taiwan
[g] Center of Infectious Disease and Signaling Research, College of Medicine, National Cheng Kung University, Tainan, Taiwan

ARTICLE INFO

Article history:
Received 5 December 2013
Received in revised form 11 February 2014
Accepted 7 April 2014

Keywords:
NSCLC
CCRT
Vinorelbine
JNK
Ceramide

ABSTRACT

The standard treatment regimen for patients diagnosed with non-small cell lung cancer (NSCLC) with locally advanced stage III disease is concurrent chemoradiotherapy (CCRT). This study investigated the molecular effects of vinca alkaloid vinorelbine (VNR)-based CCRT. We reviewed the records of 68 patients with stage III NSCLC: 42 patients received VNR-based CCRT, and 26 were treated with radiation alone. Human lung adenocarcinoma cells were used in this study to investigate the molecular effects of glucosylceramide synthase inhibition on VNR-based CCRT. There was response rate of 66.7% with CCRT, which was better than the response rate observed with radiation alone (30.8%; $P < 0.001$). CCRT caused an increase in cell cycle arrest at G_2/M phase accompanied by apoptosis. Oxidative c-Jun N-terminal kinase (JNK) activation was involved in the increased apoptosis levels but not the cell cycle arrest. CCRT also induced an increase in ceramide accompanied by a decrease in glucosylceramide that was positively correlated with the cytotoxic effects. Pharmacologically inhibiting glucosylceramide synthase facilitated VNR- and CCRT-induced apoptosis by promoting the JNK pathway. Inhibiting glucosylceramide synthase facilitates the radiosensitizing effects of VNR by promoting JNK-mediated apoptosis in lung adenocarcinoma cells.

Introduction

Lung cancer is the most common cancer worldwide. Lung cancer caused approximately 160,340 deaths in the USA in 2012 and 1,370,000 deaths worldwide in 2008 [1]. Approximately 80–85% of lung cancers are classified as non-small cell lung cancer (NSCLC), and 45% of these are diagnosed in stage III [2]. The National Comprehensive Cancer Network guidelines suggest that unresectable stage III NSCLC patients should be treated with concurrent chemoradiotherapy (CCRT), with cisplatin/etoposide or cisplatin/vinblastine plus thoracic radiation being the preferred regimens [3,4]. Randomized trials show that CCRT induces a better response rate than sequential chemotherapy (CT) and radiotherapy (RT) [5–8]. Systemic CT can reduce the chances of distant metastasis, and certain chemotherapeutic agents appear to act as radiation sensitizers. However, most of these previous trials employed multiple drugs, and toxicities from platinum-based drugs are common. The possible increased effects of CCRT have been proposed to act through several events involving increased radiation damage from the following mechanisms: the incorporation of the CT drug into DNA/RNA; interference with the DNA repair process after RT; interference with the cell cycle through cytokinetic cooperation and synchronization; enhanced activity against hypoxic cells by reoxygenation second to tumor shrinkage; RT enhancement by preventing repopulation; the inhibition of pro-survival and 'poor prognosis' markers; and hyper-radiation sensitivity [9].

Abbreviations: NSCLC, non-small cell lung cancer; CCRT, concurrent chemoradiotherapy; VNR, vinorelbine; JNK, c-Jun N-terminal kinase; CT, chemotherapy; RT, radiotherapy; NAC, N-acetyl-L-cysteine.

* Corresponding authors. Address: Institute of Clinical Medicine, College of Medicine, National Cheng Kung University, 1 University Road, Tainan 70101, Taiwan. Tel.: +886 6 2353535x4240; fax: +886 6 2758781.

E-mail addresses: Sunnysu@mail.ncku.edu.tw (W.-C. Su), cflin@mail.ncku.edu.tw (C.-F. Lin).

http://dx.doi.org/10.1016/j.canlet.2014.04.005
0304-3835/

Protocols that employ single-agent CCRT, using agents such as docetaxel [10] and gemcitabine [11], are being developed in an effort to improve patient response rates and survival. Vinorelbine (VNR) is a semi-synthetic vinca alkaloid that binds to tubulin and is a potent inhibitor of mitotic microtubule polymerization [12]. VNR is also an early and well-known radiation sensitizer [13,14] and is clinically used as a single-agent VNR-based CCRT for treatment of NSCLC [15,16]. The effects of VNR-induced radiosensitization are demonstrated by cell cycle arrest, DNA strand breaks, and apoptosis [17–21]. However, the underlying mechanisms of CCRT-induced anticancer benefits remain unclear. Our previous results demonstrate an essential role for reactive oxygen species (ROS) in VNR-induced aberrant c-Jun N-terminal kinase (JNK)-mediated Mcl-1 downregulation and DNA damage followed by mitochondrial dysfunction-related caspase-mediated apoptosis but not mitotic arrest [22]. Several reports demonstrate that radiation induces ROS accumulation, ceramide expression, DNA damage, and mitogen-activated protein kinase (MAPK) phosphorylation in different cell lines [23]. However, the increased effects caused by VNR-based CCRT lack a molecular mechanistic explanation.

Ceramide (a sphingolipid with a sphingosine backbone) levels are increased through different pathways including *de novo* synthesis, hydrolysis of sphingomyelin, and decreasing ceramide metabolism. In *de novo* synthesis, ceramide is generated from the palmitoyltransferase-mediated interaction of serine and palmitoyl-CoA and a series of metabolic reactions. In the hydrolysis pathway, extracellular stimulation induces hydrolysis of sphingolipids and sphingomyelin by sphingomyelinase. In the metabolic pathway, ceramide converts to glucosylceramide, sphingosine-1-phosphate, and ceramide-1-phosphate by glucosylceramide synthase, ceramidase, and ceramide kinase, respectively [24,25]. Exogenously and endogenously increasing ceramide levels has anticancer effects [26,27]. In the present study, we demonstrated a role for ceramide in VNR-based CCRT-induced aberrant JNK-mediated apoptosis in lung adenocarcinoma cells. We further examined a possible mechanism for ceramide expression by VNR-based CCRT and the effects of aberrant ROS/JNK and ceramide/JNK on the radiosensitizing effects of VNR in CCRT-induced apoptosis.

Materials and methods

Patients

This was a retrospective study in which we reviewed the charts of all eligible NSCLC patients from the National Cheng Kung University Hospital (NCKUH, Tainan, Taiwan) from January 1, 2005 to December 31, 2011. All information was collected by one oncology physician. The inclusion criteria were as follows: age $\geqslant$18 years; histologically documented unresectable stage III NSCLC; use of single-agent VNR–CCRT or radiation alone; adequate hematological function; and adequate liver and kidney function. The patients with impaired cognitive function were excluded. A total of 68 patients were enrolled. The adverse effects were assessed using the NCI-CTCAE version III and recorded by the physicians of the Thoracic Oncology Team. Because this study involved only chart review, the institutional review board of NCKUH agreed that informed consent was not necessary. *Clinical CCRT schedule*: Forty-two patients received CCRT, and thirty-eight patients were enrolled to calculate time to progression (TTP). Two patients received an operation immediately following CCRT, and the other two patients accepted further chemotherapy for reasons other than progression. For chemotherapy, a previous study demonstrated that 15 mg/m^2 of intravenous VNR is equivalent to 40 mg/m^2 of oral VNR [28]. Therefore, we administered a dose of 40 mg/m^2/week of oral VNR to thirty-three patients and intravenous VNR to nine patients. For radiation therapy, a computed tomography simulation-guided 3D plan was used for all patients. Intensity-modulated radiation therapy was used in 7 patients. Thoracic radiation was administered over 6 weeks at 1.8 gray (Gy) per day (for a median dose of 61.2 Gy). *Clinical radiation schedule*: Twenty-six patients received radiation alone. A computed tomography simulation-guided 3D plan was used for all patients. Thoracic radiation was administered over 6 weeks at 1.8 Gy per day (for a median dose of 60.0 Gy). *Response evaluation:* Response was evaluated with CT scans performed 4–6 weeks after completion of CCRT. According to the 2009 RECIST criteria [29], complete Response (CR) was defined as the disappearance of all target lesions. Any pathological lymph nodes (whether target or non-target) must have reduction in short axis to <10 mm. Partial Response (PR) was defined as at least a 30% decrease in the sum of diameters of target lesions taking as reference the baseline sum diameters. Progressive Disease (PD) was defined as at least a 20% increase in the sum of diameters of target lesions; taking as reference the smallest sum on study (this includes the baseline sum if that is the smallest on study). In addition to the relative increase of 20%, the sum must also demonstrate an absolute increase of at least 5 mm. (Note: the appearance of one or more new lesions is also considered progression.) Stable Disease (SD) was defined as neither sufficient shrinkage to qualify for PR nor sufficient increase to qualify for PD, taking as reference the smallest sum diameters while on study.

Cell culture and reagents

The human lung adenocarcinoma PC14PE6/AS2 cell line was established from ascites generated from PC14PE6 cells (a gift from Isaiah J. Fidler; MD Anderson Cancer Center, Houston, TX, USA) in nude mice [27]. The cells were routinely grown on plastic in Dulbecco's modified Eagle's medium (Gibco-BRL; Grand Island, NY, USA) with L-glutamine and 15 mM HEPES supplemented with 10% fetal bovine serum, 100 units/ml of penicillin, and 100 μg/ml streptomycin and maintained at 37 °C in 5% CO_2. Primary human aortic endothelial HAOEC cells were purchased from PromoCell (Heidelberg, Germany) along with the corresponding endothelial growth medium MV, which contained 0.4% human endothelial cell growth supplement, 5% fetal calf serum, 10 ng/ml epidermal growth factor, 1 μg/ml hydrocortisone, 50 ng/ml amphotericin B, and 50 μg/ml gentamicin. Other chemicals used for cell culture were purchased from Sigma–Aldrich (St. Louis, MO, USA). The vinca alkaloids VNR, vincristine, and vinblastine were purchased from Sigma–Aldrich. The JNK inhibitor SP600125, the antioxidant N-acetyl-L-cysteine (NAC), the ceramide synthase inhibitor fumonisin B1, the acid sphingomyelinase inhibitors chlorpromazine and desipramine, and the glucosylceramide synthase inhibitor D,L-*threo*-1-phenyl-2-decanoylamino-3-morpholino-1-propanol hydrochloride (PDMP) were obtained from Sigma–Aldrich and dissolved in dimethyl sulfoxide (DMSO) or ethanol prior to dilution with PBS. Rabbit anti-human MPM2, phospho-JNK (Thr183/Tyr185), JNK, PARP, and Mcl-1 antibodies were purchased from Cell Signaling Technology, Inc. (Beverly, MA, USA). Antibodies against ceramide, glucosylceramide (Glc-Ceramide), and sphingosine-1-phosphate (S-1-P) were obtained from Sigma–Aldrich. β-actin antibodies and horseradish peroxidase-conjugated or Alexa 488-conjugated anti-rabbit IgG were obtained from Chemicon International (Temecula, CA, USA).

In vitro CCRT schedule

Cells were pre-treated VNR for 24 h and the culture medium was changed before RT. Radiation was performed with 6 MV X-rays using a linear accelerator (Elekta SLi; Elekta AB, Stockholm, Sweden) at a dose of 8 Gy. We added a 5 cm of tissue-equivalent bolus on the top of a plastic tissue culture flask to guarantee electronic equilibrium, and put another 5 cm of tissue equivalent material under the flask to acquire full backscatter.

Cell cycle and apoptosis assays

Cell cycle distribution and apoptosis levels were analyzed using nuclear propidium iodide (PI; Sigma–Aldrich) staining as previously described [22] and flow cytometry (FACSCalibur; Becton Dickinson, San Jose, CA) with the excitation set at 488 nm and emission detected with the FL-2 channel (565–610 nm). The distribution of cells in the different phases of the cell cycle was calculated using MetaMorph software (Molecular Devices, Downingtown, PA). For apoptosis analysis, the samples were analyzed using CellQuest Pro 4.0.2 software (Becton Dickinson), and quantification was performed using WinMDI 2.8 software (The Scripps Institute, La Jolla, CA). Apoptosis levels are reported as the percentage (%) of cells in the sub-G_1 phase.

Intracellular ROS assay

Intracellular oxidative stress was measured using dichlorodihydrofluorescein diacetate oxidation. The cells were exposed to 20 μM 5-(and-6)-chloromethyl-2′,7′-dichlorodihydrofluorescein diacetate, acetyl ester (CM-H_2DCFDA) (Invitrogen) for 1 h. The cells were then analyzed using the FL-1 channel (515–545 nm) with a FACSCalibur cell sorter. After another wash with PBS, the cells were analyzed using flow cytometry (FACSCalibur) with an excitation wavelength of 488 nm. The ROS levels are reported as the mean fluorescence intensity (MFI) of the total cells using CellQuest Pro 4.0.2 software, and quantification was performed with WinMDI 2.8 software. Small cell debris were excluded by gating on a forward scatter plot.

Immunostaining

To detect the expression of MPM-2 and sphingolipid metabolites, we fixed, stained, and analyzed the cells as described elsewhere [30]. Briefly, the cells were fixed and permeabilized with 3.7% formaldehyde in PBS. After the cells were washed and stained with primary antibody followed by an Alexa 488-conjugated secondary antibody, the cells were analyzed using flow cytometry (FACSCalibur).

Western blot analysis

The harvested cells were prepared and analyzed for protein expression as described elsewhere [30]. The relative signal intensity was quantified using ImageJ software (version 1.41o) from W. Rasband (National Institutes of Health, Bethesda, MD). The changes in the ratio of proteins compared with the normalized value of untreated cells (indicated protein/β-actin or phosphorylated protein/total protein/β-actin) were also shown.

Statistical analysis

The values are given as the mean ± standard deviation (SD). The groups were compared using Student's two-tailed unpaired *t* test; significance was set at *P*-value <0.05.

Results

VNR-based CCRT has superior effects over radiation alone

On average, 330 patients per year are diagnosed with lung cancer at the NCKUH, and 19% of these patients (64 patients per year) have stage III disease. Approximately 15–20 patients per year present with unresectable stage III NSCLC without malignant pleural effusion, and 6 patients per year receive CCRT. From January 1, 2005 to December 31, 2011, 42 patients were treated with VNR single-agent CCRT, and 26 patients were treated with radiation alone. We excluded two patients because surgery was performed after CCRT, and an additional two patients were excluded because they were immediately given taxane therapy. Ultimately, we included 38 CCRT patients for TTP calculations (Table 1). In the CCRT group, the median TTP was 196 days (approximately 6.5 months); in the radiation group, the median TTP was 177 days (approximately 6 months; $p = 0.029$). One patient had a complete response (CR, 2.4%), and 27 patients had partial responses (PR, 64.3%) in the CCRT group. The objective response rate (CR + PR) for all 42 patients was 66.7%; the response rate was 30.8% (8/26) in the radiation group ($p < 0.001$). The median survival time was 570 days in the CCRT group and 415 days in the radiation group ($p = 0.175$). As summarized in Table 2, variables significantly different between the two groups were age ($p < 0.001$), performance ($p < 0.001$), TTP ($p = 0.029$), dysphagia ($p < 0.001$), dermatitis ($p = 0.006$), and leukopenia ($p < 0.001$). These results show a benefit response in VNR-based CCRT with respect to radiation alone.

CCRT facilitates cell cycle arrest at the G_2/M phase followed by JNK-regulated apoptosis in human lung adenocarcinoma cells

Treatment with VNR causes apoptosis following cell cycle arrest at the G_2/M phase in human lung adenocarcinoma PC14PE6/AS2 and A549 cells [22], and RT also induces G_2/M phase arrest and apoptosis [23]. In this study, we investigated the increased effects of CCRT on cell cycle progression and apoptosis in PC14PE6/AS2 cells. Nuclear PI staining followed by flow cytometry revealed that CCRT significantly ($p < 0.01$) induced a G_2/M arrest compared to VNR-based CT or RT treatment alone (Fig. 1A). To further characterize the specific phase arrest, the expression of MPM2, a mitotic phase marker [16], was determined using flow cytometry. The results showed that a high dose of CT (100 nM) caused a significant ($p < 0.01$) increase in mitotic arrest. However, CCRT significantly ($p < 0.001$) diminished CT-induced mitotic arrest (Fig. 1B). We previously showed that VNR causes mitotic arrest followed by apoptosis [22]. Here, apoptosis analysis demonstrated that CCRT significantly ($p < 0.001$) induced cell death in an increased manner compared to VNR-based CT- or RT-treated cells (Fig. 1C). We next investigated the increased effects of CCRT on G_2/M arrest and apoptosis in human aortic endothelial HAOEC cells because tumors are composed of cancer cells and vessels. Consistent with the cancer cell response, apoptosis analysis showed that CCRT significantly ($p < 0.001$) induced G_2/M arrest and apoptosis (supplementary Fig. 1). These results demonstrate that CCRT facilitates G_2/M arrest followed by apoptosis.

MAPKs are primarily affected by vinca alkaloids [31], and VNR induces JNK-regulated Mcl-1 downregulation followed by mitochondrial apoptosis [22]. Therefore, we next examined the role of JNK in CCRT-induced toxicity. Western blot analysis showed that CCRT partly increased JNK phosphorylation (Thr183/Tyr185) accompanied by an increase in apoptosis, as shown by PARP cleavage (Fig. 1D). PI staining-based flow cytometric analysis also demonstrated that JNK inhibition by SP600125 treatment did not reduce the CCRT-induced G_2/M arrest (Fig. 1E) but significantly ($p < 0.01$) diminished CCRT-induced apoptosis (Fig. 1F). Protein analysis showed that treatment with SP600125 effectively decreased CCRT-induced Mcl-1 downregulation and PARP cleavage (Fig. 1G). These findings indicate JNK plays a key role in apoptosis induced by CCRT but not G_2/M arrest, partly through Mcl-1 downregulation.

ROS facilitate JNK activation in CCRT-induced apoptosis

We next examined the role of ROS in CCRT-induced apoptosis and activation of apoptosis signaling kinase 1/JNK activation [22]. CM-H_2DCFDA staining followed by flow cytometry demonstrated that CCRT significantly ($p < 0.001$) induced ROS generation compared to CT or RT treatment alone (Fig. 2A). The antioxidant agent NAC was added to block ROS generation. Nuclear PI staining followed by flow cytometry showed that blocking ROS partially but significantly ($p < 0.001$) reduced CCRT-induced apoptosis (Fig. 2B). Western blotting further revealed that NAC effectively

Table 1
Comparing response rate, TTP, and survive between patients received CCRT or radiation alone.

Treatment (patient number)	CCRT (38/42)[a]	RT (26)	*p* Value
Response rate [CR + PR]	66.7% (28/42) [2.4% + 64.3%]	30.8% (8/26) [0% + 30.8%]	<0.001
TTP, mean/median days	299/196 (38)	162.2/177	0.029
Survive days, mean/median days	796/570 (42)	590/415	0.175
Follow up days	532	396	<0.001

[a] We excluded two patient because they received surgery after CCRT, and an additional two patients who were given taxanes therapy immediately.

Table 2
Characteristics and toxicities between patients received CCRT or radiation.

Treatment (patient number)	CCRT (42)	RT (26)	*p* Value
T1/T2/T3/T4	3/13/12/14	2/7/4/13	0.446
N0/N1/N2/N3	1/1/23/17	2/2/16/6	0.080
IIIA/IIIB	16/26	7/19	0.343
Age (mean/median)	70/72	78/80	<0.001
Female/male	6/36	4/22	0.904
Smoking ±	13/29	7/19	0.726
VNR oral/intravenous	31/11		
VNR cycles (mean/median)	6/6		
ECOG 0/1/2/3	16/20/5/1	0/12/9/4 M:1	<0.001
RT dose (median Gy)	6120	6000	0.114
RT fractions (mean/median)	32/34	30/30	0.171
Progression	31	18	0.692
Death	22	15	0.675
Pathology N/A/S/L	5/20/16/1	7/5/14/0	0.844
Pneumonitis ±	15/17	17/9	0.928
Dysphagia Grade 0/1/2/3	16/14/11/1	17/9/0/0	<0.001
Dermatitis Grade 0/1/2	27/10/5	23/3/0	0.006
Leukopenia Grade 0/1/2/3	32/1/8/1	0/0/0/0	<0.001

TNM: 2009 TNM staging system; ECOG: Eastern Cooperative Oncology Group performance scale; M: missing data; pathology N/A/S/L: non-small cell carcinoma/adenocarcinoma/squamous cell carcinoma/large cell carcinoma; toxicities grade: dysphagia, dermatitis, and leucopenia grade according to NCI-CTCAE version III.

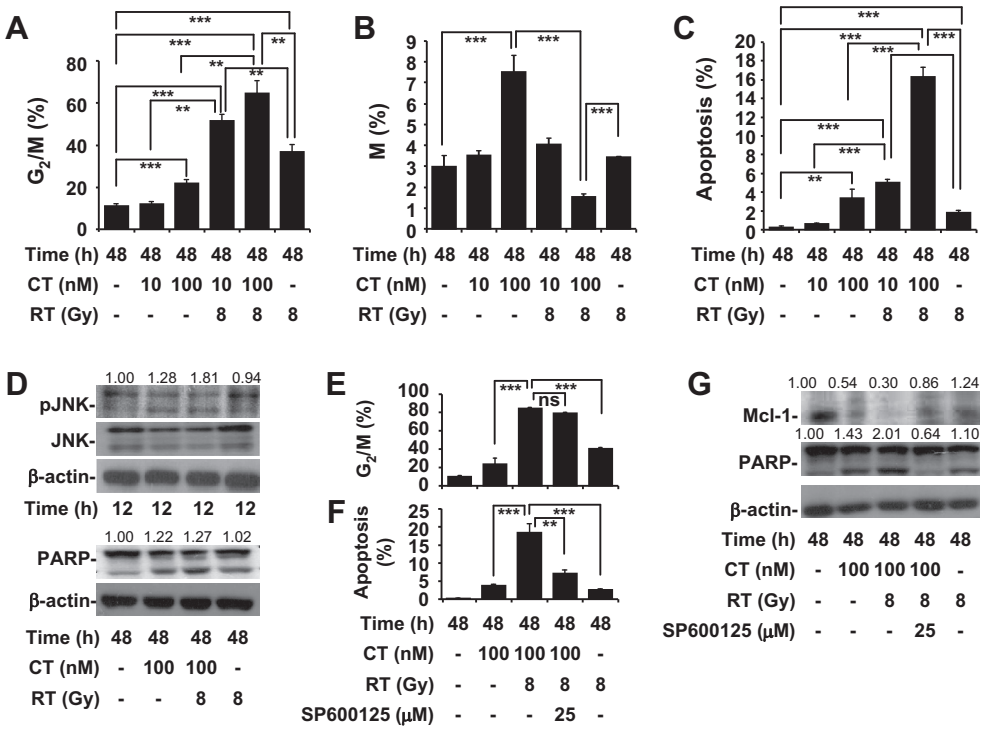

Fig. 1. CCRT increases cell cycle arrest at G_2/M phase followed by JNK-regulated apoptosis in human lung adenocarcinoma cells. Nuclear PI plus MPM-2 staining and subsequent flow cytometric analysis were used to determine cell cycle at G_2/M (A) or mitotic (M) phase (B) and cell apoptosis (C) in VNR-based chemotherapy (CT)-, radiotherapy (RT)-, or CCRT-treated PC14PE6/AS2 cells. The percentages (%) of positive cells are shown as the mean ± SD of three individual experiments. $^{**}p < 0.01$ and $^{***}p < 0.001$. (D) Western blot showing the expression of phospho-JNK (pJNK), JNK, and PARP in VNR-based chemotherapy (CT)-, radiotherapy (RT)-, or CCRT-treated PC14PE6/AS2 cells. Nuclear PI staining and subsequent flow cytometric analysis were used to determine the cell cycle at G_2/M phase (E) and apoptosis (F) in CT-, RT-, or CCRT-treated PC14PE6/AS2 cells with or without co-treatment with the JNK inhibitor SP600125. The percentages (%) of positive cells are shown as the mean ± SD of three individual experiments. ns, not significant. $^{**}p < 0.01$ and $^{***}p < 0.001$. (G) Western blot showing the expression levels of Mcl-1 and PARP. β-actin was used as an internal control. The changes in the ratio of the measured proteins compared with the normalized value of untreated cells are also shown. One representative dataset obtained from three individual experiments is shown.

decreased CCRT-induced JNK phosphorylation (Thr183/Tyr185; Fig. 2C). Data indicate ROS partially facilitate CCRT-induced apoptosis through JNK activation.

CCRT increases ceramide expression accompanied by a decrease in glucosylceramide

RT induces ROS generation accompanied by ceramide expression in different cell types [23]. Because the pro-apoptotic role of ceramide has also been demonstrated after RT, we next examined the involvement of ceramide signaling in CCRT. Ceramide immunostaining followed by flow cytometry showed that CCRT significantly ($p < 0.001$) induced ceramide expression compared to CT or RT treatment alone (Fig. 3A, top and supplementary Fig. 2, top). We also investigated the levels of glucosylceramide and sphingosine-1-phosphate (S-1-P) because these sphingolipid metabolites are typically regulated during ceramide expression [24,25]. Surprisingly, CCRT significantly ($p < 0.001$) decreased glucosylceramide generation compared to CT alone (Fig. 3A, middle and supplementary Fig. 2, middle), but there were no changes in the S-1-P levels (Fig. 3A, bottom and supplementary Fig. 2, bottom). To clarify the potential effects of ceramide expression on

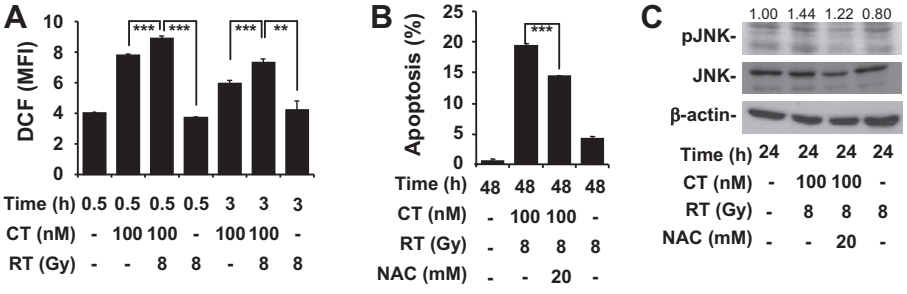

Fig. 2. CCRT induces oxidative JNK-regulated apoptosis. (A) CM-H_2DCFDA staining showing ROS levels in VNR-based chemotherapy (CT)-, radiotherapy (RT)-, or CCRT-treated PC14PE6/AS2 cells. The mean fluorescence intensity (MFI) of each stain is shown as the mean ± SD of three individual experiments. $^{**}p < 0.01$ and $^{***}p < 0.001$. (B) Nuclear PI staining and subsequent flow cytometric analysis was used to determine apoptosis in CCRT-treated PC14PE6/AS2 cells with co-treatment with the antioxidant NAC. The percentages (%) of apoptotic cells are shown as the means ± SD of three individual experiments. $^{***}p < 0.001$. (C) Western blot showing the expression of phospho-JNK (pJNK) and JNK. β-actin was used as an internal control. The changes in the ratio of the measured proteins compared with the normalized value of untreated cells are also shown. One representative dataset obtained from repeated experiments is shown.

CCRT-induced apoptosis, fumonisin B1 (a ceramide synthase inhibitor) and chlorpromazine and desipramine (acidic sphingomyelinase inhibitors) were used. However, inhibiting ceramide expression by blocking the *de novo* synthesis- and hydrolysis-regulated pathways did not alter CT- or RT-induced apoptosis (Fig. 3B and C) or CCRT-induced apoptosis (Fig. 3D), as determined using nuclear PI staining followed by flow cytometry. The effects of CCRT on ceramide metabolism and apoptosis (supplementary Fig. 3) were confirmed in A549 cells. To verify whether the synthesis- and the hydrolysis-regulated pathways are required for the generation of ceramide by CCRT, we next checked their roles using a pharmacological approach. Our results demonstrated an independent role of them in CCRT-induced ceramide generation (Fig. 3E). These findings suggest that CCRT causes an increase in ceramide expression and apoptosis, and CCRT inhibits glucosylceramide generation.

Blockage of glucosylceramide synthase facilitates CCRT-induced JNK-regulated apoptosis

To further evaluate the possible role of glucosylceramide synthase inhibition by CCRT, we hypothesized that the ceramide was accumulated from the halt of glucosylceramide metabolism [24]. Treatment with PDMP [30], a glucosylceramide inhibitor, significantly ($p < 0.001$) enhanced ceramide generation (supplementary Fig. 4) and apoptosis in VNR-based CT- (Fig. 4A) and CCRT – (Fig. 4C) but not RT – (Fig. 4B) treated cells, as shown using nuclear PI staining followed by flow cytometry. In addition to VNR, PDMP treatment also enhanced other vinca alkaloid-based (vincristine and vinblastine) CT-induced apoptosis in PC14PE6/AS2 cells (supplementary Fig. 5). JNK inhibition through SP600125 treatment significantly ($p < 0.001$) diminished CT-induced (Fig. 4D) and CCRT-enhanced (Fig. 4E) apoptosis under

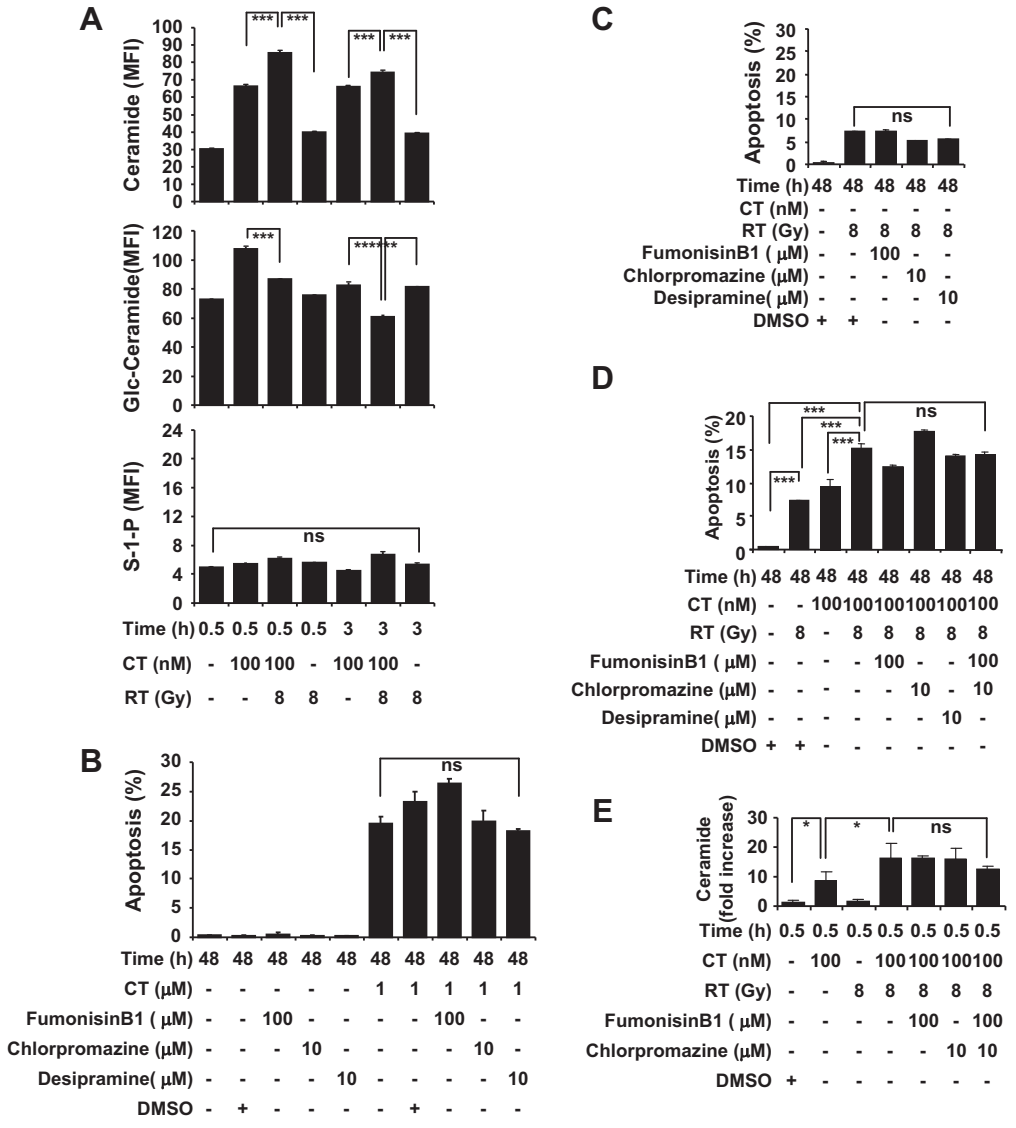

Fig. 3. CCRT causes an increase in ceramide expression accompanied by glucosylceramide inhibition. (A) Immunostaining followed by flow cytometric analysis showing the levels of ceramide, glucosylceramide (Glc-ceramide), and sphingosine-1-phosphate (S-1-P) in PC14PE6/AS2 cells treated with VNR-based chemotherapy (CT), radiotherapy (RT), or CCRT. The mean fluorescence intensity (MFI) of each stain is shown as the mean ± SD of three individual experiments. ns, not significant. $^{***}p < 0.001$. Nuclear PI staining and subsequent flow cytometric analysis were used to determine cell apoptosis in CT- (B), RT- (C), or CCRT- (D) treated PC14PE6/AS2 cells with co-treatment with the *de novo* ceramide synthase inhibitor fumonisin B1 and acid sphingomyelinase inhibitors chlorpromazine and desipramine. DMSO was used as a negative control. The percentages (%) of apoptotic cells are shown as the means ± SD of three individual experiments. (E) Meanwhile, ceramide immunostaining showed the generation of ceramide in CCRT-treated cells. Data (means ± SD of triplicate cultures) are shown as a fold change compared with the normalized value of control. ns, not significant. $^{**}p < 0.01$ and $^{***}p < 0.001$.

PDMP treatment. CM-H_2DCFDA staining followed by flow cytometry demonstrated that PDMP significantly ($p < 0.001$) enhanced CT-induced ROS generation (supplementary Fig. 6A). ROS inhibition by NAC also partially but significantly ($p < 0.001$) reduced PDMP-enhanced CCRT-induced apoptosis (supplementary Fig. 6B). Western blotting showed that NAC treatment partially decreased CCRT-induced JNK phosphorylation (Thr183/Tyr185) in PDMP-treated cells (Fig. 4F). The data indicate glucosylceramide synthase inhibition facilitates CCRT-induced apoptosis through JNK activation.

Discussion

This translational research included clinical association and basic research to investigate molecular mechanisms for CCRT. Combined modality therapy has superior disease control over radiation alone in stage III NSCLC patients [32]. Our former report demonstrates that single-agent VNR CCRT results in improved median survival times and 2-year survival rates with less toxicity compared to other therapies [16]. Consistent with the previous studies [5–8], in this retrospective study, we observed that the TTP was extended in CCRT patients compared to radiation patients. However, survival was not significantly different. We hypothesized that TTP could represent the true response effects because survival is affected by other chemotherapy regimens. Older and poorer performance patients were noted in the CCRT group, indicating that VNR-based CCRT is suitable for the treatment of elderly patients with a poor performance status. CCRT patients suffered from more side effects, especially dysphagia and dermatitis. We used a lower VNR dose with reduced toxicity levels than another phase I study in elderly patients [15]. Large prospective phase III trials are necessary to verify our findings.

For the treatment of NSCLC patients who are generally in the final stages, CCRT has a better therapeutic advantage over CT and RT individually by potentiating tumor growth inhibition and cancer cell apoptosis [9]. In support of the radiosensitization of VNR, increases in cell cycle arrest (mostly at G_2/M phase), DNA strand breaks, and apoptosis levels have been demonstrated in VNR-based CCRT-treated lung cancer cell lines *in vitro*, including NCI-H460, A549, PC-9, SBC-3, and H292 cells [17–21]. However, the exact molecular mechanism remains unknown. To investigate the mechanisms of the increased effects, human lung adenocarcinoma PC14PE6/AS2 cells, an NSCLC cell line with highly metastatic properties [27], were exposed to VNR-based CCRT treatment. Consistent with the above studies in lung cancer cells, the effects of VNR-induced radiosensitization were commonly associated with G_2/M arrest and cell apoptosis. While DNA damage was also identified and enhanced by CCRT (data not shown), DNA damage-associated p53 and ATR/ATM activation can be excluded as factors in PC14PE6/AS2 cells because these cells contain a loss-of-function p53 mutation, and ATR/ATM inhibition does not reduce VNR-induced G_2/M arrest or apoptosis [22]. Furthermore, p53 was silenced in another human NSCLC cell line, A549 cells, and the results demonstrate that VNR causes G_2/M arrest and apoptosis in a p53-independent manner [22]. According to our findings in PC14PE6/AS2 cells, we speculate that p53 is not involved in the CCR-induced effects in our experimental model. The actual involvement of DNA damage for the radiosensitization effects of VNR requires further investigation.

While investigating the molecular mechanisms of the VNR radiosensitizing effects, it is notable that vinca alkaloids cause ROS-mediated JNK activation, Mcl-1 downregulation, and apoptosis in PC14PE6/AS2 cells [22]. Although JNK activation partially determines DNA damage and apoptosis, VNR-induced cell cycle

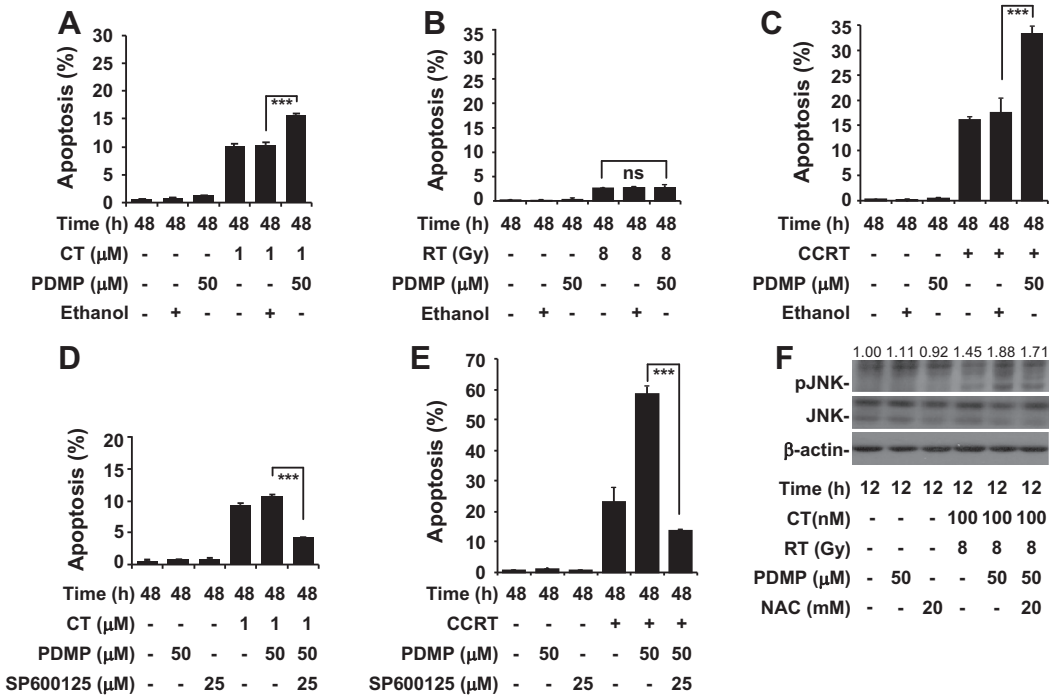

Fig. 4. Pharmacologically inhibiting glucosylceramide synthase facilitates CT- and CCRT-induced apoptosis through the JNK-regulated pathway. Nuclear PI staining and subsequent flow cytometric analysis were used to determine cell apoptosis in VNR-based chemotherapy (CT)- (A), radiotherapy (RT)- (B), or CCRT- (C) treated PC14PE6/AS2 cells with co-treatment with the glucosylceramide synthase inhibitor PDMP and CT plus PDMP- (D) or CCRT plus PDMP- (E) treated PC14PE6/AS2 cells with co-treatment with the JNK inhibitor SP600125. The percentages (%) of positive cells are shown as the mean ± SD of three individual experiments. ns, not significant. $^{***}p < 0.001$. (F) Western blot showing the expression of phospho-JNK (pJNK) and JNK in CCRT plus PDMP-treated PC14PE6/AS2 cells with co-treatment with the antioxidant NAC. β-actin was used as an internal control. The changes in the ratio of the measured proteins compared with the normalized value of untreated cells are also shown. One representative dataset obtained from repeated experiments is shown.

arrest at G_2/M phase is JNK-independent. In addition to CT, RT also induces ROS accumulation, ceramide expression, DNA damage and MAPK phosphorylation in different cell lines [23]. According to the results of this study, as summarized in supplementary Fig. 7, CCRT induces an increased response by enhancing a JNK-independent G_2/M arrest accompanied by apoptosis through ceramide- and ROS-regulated JNK activation. To our knowledge, this is the first study to determine a molecular mechanism that explains the increased effects of the radiosensitizer VNR in CCRT.

JNK activation mediates apoptosis in lung cancer cells following VNR treatment [22]. For JNK activation, oxidative stress induced by aberrant ROS generation activates the apoptosis signaling kinase 1/MAPK kinase 4/7/JNK axis signaling in VNR-treated cells, as well as in other cells in response to apoptotic stimuli [33,34]. Importantly, ROS generation is associated with the aberrant accumulation of mitochondria in VNR-treated cells arrested at M phase [22]. In addition to ROS, previous studies report that ceramide can activate JNK to mediate apoptotic pathways before mitochondrial injury in lung cancer cells [35,36]. In addition, the molecular action of ceramide-activated JNK may also be indirectly regulated by ROS. Consistent with these findings, CCRT-facilitated apoptosis is mediated by a JNK-regulated mechanism by enhancing ROS generation following G_2/M arrest and ceramide expression. To explore the VNR radiosensitization, the downstream signaling pathways of JNK-mediated apoptosis, such as Mcl-1 downregulation and Bim activation [36,37], require further investigation.

Ceramide acts as a signal transducer for apoptosis in response to RT [23] and CT [38,39]. However, little is known regarding CCRT and the complicated crosstalk involved in the increased effects. This study showed that VNR causes ceramide expression independent of *de novo* synthesis or sphingomyelinase-mediated hydrolysis pathways. Further studies revealed that ROS inhibition did not alter ceramide expression (supplementary Fig. 8). In contrast, ceramide acted upstream of ROS generation, and this regulation requires further study. Surprisingly, CCRT facilitated ceramide expression following glucosylceramide decrease. However, this result was inconsistent with the data that VNR alone increases ceramide accompanied by the accumulation of its metabolite glucosylceramide. We therefore hypothesize that CCRT facilitates ceramide expression by altering ceramide metabolism forward to glucosylceramide through the inhibition of the enzymatic activity of glucosylceramide synthase. The principal question raised from this hypothesis is how CCRT causes such effects, while our study only indicated that ROS does not affect ceramide expression. Further investigation of glucosylceramide synthase inhibition is needed.

Ceramide generation can be modulated exogenously by administering ceramide analogues and endogenously by inhibiting ceramide metabolism through inhibition of ceramidase and glucosylceramide synthase [24–26]. Our current study demonstrated that treating leukemia cells with PDMP, an inhibitor of glucosylceramide synthase, increases cell apoptotic susceptibility in response to the anticancer agents imatinib and nilotinib [30]. Consistent with this approach, based on the results of this study, pharmacologically blocking glucosylceramide synthesis using PDMP facilitates both VNR- and CCRT-induced apoptosis. A genetic approach is currently under investigation to confirm such findings in this study. Notably, the multidrug resistance (MDR) of vinca alkaloids has been previously mentioned in several cancers with the aberrant regulation of glucosylceramide synthase, which causes ceramide metabolism to avoid ceramide-induced apoptosis [40]. According to our findings, VNR-based CCRT and/or combined PDMP treatment may both facilitate anticancer activity and overcome the cancer MDR of VNR by inhibiting glucosylceramide synthase. In addition to VNR, the radiosensitizing effects of PDMP combined therapy are therefore suggested for anticancer therapy in the near future.

In conclusion, VNR-based CCRT has superior disease control compared to RT or CT alone. The findings of this study shed light on the radiosensitization and the molecular basis of VNR-based CCRT, which is facilitated by JNK activation following ceramide- and ROS-regulated mechanisms. Generation of ceramide may result from CCRT-induced glucosylceramide synthase inhibition. With CCRT, JNK-independent G_2/M arrest and JNK-regulated apoptosis were demonstrated in this study. We also provide a strategy to simultaneously increase the anticancer activity of CT and CCRT by modulating ceramide expression.

Conflict of Interest

The authors declare no conflict of interest.

Acknowledgements

We thank the Immunobiology Core of the Research Center of Clinical Medicine at the National Cheng Kung University Hospital, College of Medicine, National Cheng Kung University, Tainan, Taiwan, for providing services that include training, technical support, and assistance with experimental design and data analysis using the Flow Cytometry Core facilities. This work was supported by grants NCKUH-10103035 from the National Cheng Kung University Hospital in Taiwan and NSC100-2320-B-006-009-MY3 from the National Science Council, Taiwan.

Appendix A. Supplementary material

Supplementary data associated with this article can be found, in the online version, at http://dx.doi.org/10.1016/j.canlet.2014.04.005.

References

[1] R. Siegel, D. Naishadham, A. Jemal, Cancer statistics, CA Cancer J. Clin. 62 (2012) 10–29.
[2] H. Bulzebruck, R. Bopp, P. Drings, E. Bauer, S. Krysa, G. Probst, G. van Kaick, K.M. Muller, I. Vogt-Moykopf, New aspects in the staging of lung cancer. Prospective validation of the International Union Against Cancer TNM classification, Cancer 70 (1992) 1102–1110.
[3] G.M. Videtic, Locally advanced non-small cell lung cancer: what is the optimal concurrent chemoradiation regimen?, Cleveland Clinic J Med. 79, Electronic Suppl 1 (2012) eS32–eS37.
[4] M. Provencio, D. Isla, A. Sanchez, B. Cantos, Inoperable stage III non-small cell lung cancer: current treatment and role of vinorelbine, J. Thoracic Dis. 3 (2011) 197–204.
[5] C. Schaake-Koning, W. van den Bogaert, O. Dalesio, J. Festen, J. Hoogenhout, P. van Houtte, A. Kirkpatrick, M. Koolen, B. Maat, A. Nijs, et al., Effects of concomitant cisplatin and radiotherapy on inoperable non-small-cell lung cancer, N. Engl. J. Med. 326 (1992) 524–530.
[6] B. Jeremic, Y. Shibamoto, L. Acimovic, L. Djuric, Randomized trial of hyperfractionated radiation therapy with or without concurrent chemotherapy for stage III non-small-cell lung cancer, J. Clin. Oncol. 13 (1995) 452–458.
[7] R.O. Dillman, J. Herndon, S.L. Seagren, W.L. Eaton Jr., M.R. Green, Improved survival in stage III non-small-cell lung cancer: seven-year follow-up of cancer and leukemia group B (CALGB) 8433 trial, J. Natl. Cancer Inst. 88 (1996) 1210–1215.
[8] W. Sause, P. Kolesar, S.I. Taylor, D. Johnson, R. Livingston, R. Komaki, B. Emami, W. Curran Jr., R. Byhardt, A.R. Dar, A. Turrisi 3rd, Final results of phase III trial in regionally advanced unresectable non-small cell lung cancer: radiation therapy oncology group, eastern cooperative oncology group, and southwest oncology group, Chest 117 (2000) 358–364.
[9] T.Y. Seiwert, J.K. Salama, E.E. Vokes, The concurrent chemoradiation paradigm–general principles, Nat. Clin. Pract. Oncol. 4 (2007) 86–100.
[10] H. Onishi, K. Kuriyama, M. Yamaguchi, T. Komiyama, S. Tanaka, T. Araki, K. Nishikawa, H. Ishihara, Concurrent two-dimensional radiotherapy and weekly docetaxel in the treatment of stage III non-small cell lung cancer: a good local response but no good survival due to radiation pneumonitis, Lung Cancer 40 (2003) 79–84.
[11] D. Galetta, A. Cesario, S. Margaritora, V. Porziella, A. Piraino, R.M. D'Angelillo, M.A. Gambacorta, S. Ramella, L. Trodella, S. Valente, G.M. Corbo, G. Macis, A. Mule, V. Cardaci, S. Sterzi, P. Granone, P. Russo, Multimodality treatment of unresectable stage III non-small cell lung cancer: interim analysis of a phase II

trial with preoperative gemcitabine and concurrent radiotherapy, J. Thorac. Cardiovasc. Surg. 131 (2006) 314–321.
[12] V.K. Ngan, K. Bellman, D. Panda, B.T. Hill, M.A. Jordan, L. Wilson, Novel actions of the antitumor drugs vinflunine and vinorelbine on microtubules, Cancer Res. 60 (2000) 5045–5051.
[13] H.A. Burris 3rd, S. Fields, Summary of data from in vitro and phase I vinorelbine (Navelbine) studies, Seminars Oncol. 21 (1994) 14–19. discussion 19–20.
[14] M. Candelaria, A. Garcia-Arias, L. Cetina, A. Duenas-Gonzalez, Radiosensitizers in cervical cancer. Cisplatin and beyond, Radiat. Oncol. 1 (2006) 15.
[15] H. Harada, T. Seto, S. Igawa, A. Tsuya, M. Wada, K. Kaira, T. Naito, K. Hayakawa, T. Nishimura, N. Masuda, N. Yamamoto, Phase I results of vinorelbine with concurrent radiotherapy in elderly patients with unresectable, locally advanced non-small-cell lung cancer: West Japan Thoracic Oncology Group (WJTOG3005-DI), Int. J. Radiat. Oncol., Biol., Phys. 82 (2012) 1777–1782.
[16] W.H. Chiu, H.W. Chen, W.C. Su, Oral vinorelbine: a better choice for concurrent chemoradiotherapy in stage III non-small cell lung cancer, J. Solid Tumors 2 (2012) 4–15.
[17] M.P. Edelstein, L.A. Wolfe 3rd, D.S. Duch, Potentiation of radiation therapy by vinorelbine (Navelbine) in non-small cell lung cancer, Sem. Oncol. 23 (1996) 41–47.
[18] K. Fukuoka, H. Arioka, Y. Iwamoto, H. Fukumoto, H. Kurokawa, T. Ishida, A. Tomonari, T. Suzuki, J. Usuda, F. Kanzawa, N. Saijo, K. Nishio, Mechanism of the radiosensitization induced by vinorelbine in human non-small cell lung cancer cells, Lung Cancer 34 (2001) 451–460.
[19] K. Fukuoka, H. Arioka, Y. Iwamoto, H. Fukumoto, H. Kurokawa, T. Ishida, A. Tomonari, T. Suzuki, J. Usuda, F. Kanzawa, H. Kimura, N. Saijo, K. Nishio, Mechanism of vinorelbine-induced radiosensitization of human small cell lung cancer cells, Cancer Chemother. Pharmacol. 49 (2002) 385–390.
[20] M. Zhang, M. Boyer, L. Rivory, A. Hong, S. Clarke, G. Stevens, K. Fife, Radiosensitization of vinorelbine and gemcitabine in NCI-H460 non-small-cell lung cancer cells, Int. J. Radiat. Oncol., Biol., Phys. 58 (2004) 353–360.
[21] C. Simoens, F. Lardon, B. Pauwels, C.M. De Pooter, H.A. Lambrechts, G.G. Pattyn, F. Breillout, J.B. Vermorken, Comparative study of the radiosensitizing and cell cycle effects of vinflunine and vinorelbine, in vitro, BMC Cancer 8 (2008) 65.
[22] W.H. Chiu, S.J. Luo, C.L. Chen, J.H. Cheng, C.Y. Hsieh, C.Y. Wang, W.C. Huang, W.C. Su, C.F. Lin, Vinca alkaloids cause aberrant ROS-mediated JNK activation, Mcl-1 downregulation, DNA damage, mitochondrial dysfunction, and apoptosis in lung adenocarcinoma cells, Biochem. Pharmacol. 83 (2012) 1159–1171.
[23] R.K. Schmidt-Ullrich, Molecular targets in radiation oncology, Oncogene 22 (2003) 5730–5733.
[24] W.C. Huang, C.L. Chen, Y.S. Lin, C.F. Lin, Apoptotic sphingolipid ceramide in cancer therapy, J. Lipids 2011 (2011) 565316.
[25] Y.A. Hannun, L.M. Obeid, Many ceramides, J. Biol. Chem. 286 (2011) 27855–27862.
[26] C.F. Lin, C.L. Chen, Y.S. Lin, Ceramide in apoptotic signaling and anticancer therapy, Curr. Med. Chem. 13 (2006) 1609–1616.
[27] C.S. Anderson, W.J. Curran, Combined modality therapy for stage III non-small-cell lung cancer, Sem. Radiat. Oncol. 20 (2010) 186–191.
[28] G. Beckmann, R. Fietkau, R.M. Huber, P. Kleine, M. Schmidt, S. Semrau, D. Aubert, A. Fittipaldo, M. Flentje, Oral vinorelbine and cisplatin with concomitant radiotherapy in stage III non-small cell lung cancer (NSCLC): a feasibility study, Onkologie 29 (2006) 137–142.
[29] E.A. Eisenhauer, P. Therasse, J. Bogaerts, L.H. Schwartz, D. Sargent, R. Ford, J. Dancey, S. Arbuck, S. Gwyther, M. Mooney, L. Rubinstein, L. Shankar, L. Dodd, R. Kaplan, D. Lacombe, J. Verweij, New response evaluation criteria in solid tumours: revised RECIST guideline (Version 1.1), Eur. J. Cancer 45 (2009) 228–247.
[30] W.C. Huang, C.C. Tsai, C.L. Chen, T.Y. Chen, Y.P. Chen, Y.S. Lin, P.J. Lu, C.M. Lin, S.H. Wang, C.W. Tsao, C.Y. Wang, Y.L. Cheng, C.Y. Hsieh, P.C. Tseng, C.F. Lin, Glucosylceramide synthase inhibitor PDMP sensitizes chronic myeloid leukemia T315I mutant to Bcr-Abl inhibitor and cooperatively induces glycogen synthase kinase-3-regulated apoptosis, FASEB J.: Official Publ. Federation Am. Soc. Exp. Biol. 25 (2011) 3661–3673.
[31] A.A. Stone, T.C. Chambers, Microtubule inhibitors elicit differential effects on MAP kinase (JNK, ERK, and p38) signaling pathways in human KB-3 carcinoma cells, Exp. Cell Res. 254 (2000) 110–119.
[32] T.E. Stinchcombe, D. Fried, D.E. Morris, M.A. Socinski, Combined modality therapy for stage III non-small cell lung cancer, Oncologist 11 (2006) 809–823.
[33] K. Tobiume, A. Matsuzawa, T. Takahashi, H. Nishitoh, K. Morita, K. Takeda, O. Minowa, K. Miyazono, T. Noda, H. Ichijo, ASK1 is required for sustained activations of JNK/p38 MAP kinases and apoptosis, EMBO Rep. 2 (2001) 222–228.
[34] J. Wang, J. Yi, Cancer cell killing via ROS: to increase or decrease, that is the question, Cancer Biol. Ther. 7 (2008) 1875–1884.
[35] P.P. Ruvolo, Intracellular signal transduction pathways activated by ceramide and its metabolites, Pharmacol. Res. 47 (2003) 383–392.
[36] S.M. Kurinna, C.C. Tsao, A.F. Nica, T. Jiffar, P.P. Ruvolo, Ceramide promotes apoptosis in lung cancer-derived A549 cells by a mechanism involving c-Jun NH2-terminal kinase, Cancer Res. 64 (2004) 7852–7856.
[37] S. Inoshita, K. Takeda, T. Hatai, Y. Terada, M. Sano, J. Hata, A. Umezawa, H. Ichijo, Phosphorylation and inactivation of myeloid cell leukemia 1 by JNK in response to oxidative stress, J. Biol. Chem. 277 (2002) 43730–43734.
[38] L.M. Obeid, C.M. Linardic, L.A. Karolak, Y.A. Hannun, Programmed cell death induced by ceramide, Science 259 (1993) 1769–1771.
[39] R. Bose, M. Verheij, A. Haimovitz-Friedman, K. Scotto, Z. Fuks, R. Kolesnick, Ceramide synthase mediates daunorubicin-induced apoptosis: an alternative mechanism for generating death signals, Cell 82 (1995) 405–414.
[40] Y.Y. Liu, T.Y. Han, A.E. Giuliano, M.C. Cabot, Ceramide glycosylation potentiates cellular multidrug resistance, FASEB J.: Official Publ. Federation Am. Soc. Exp. Biol. 15 (2001) 719–730.